

# ON POSITRON BEAM DYNAMICS IN AN INITIAL PART OF A LARGE APERTURE FCC-EE CAPTURE LINAC\*

V. Mytrochenko<sup>1,3†</sup>, F. Alharthi<sup>1</sup>, A. Bacci<sup>2</sup>, E. Bulyak<sup>3</sup>, I. Chaikovska<sup>1</sup>, R. Chehab<sup>1</sup>, M. Rossetti<sup>2</sup>

<sup>1</sup>Université Paris-Saclay, CNRS/IN2P3, IJCLab, 91405 Orsay, France

<sup>2</sup>INFN, Milano, Lombardia, Italia

<sup>3</sup>NSC KIPT, Kharkiv, 61108, Ukraine

## Abstract

The application of HTS coils for a matching device [1] and a large-aperture L-band linac [2] makes it possible to transport a substantial part of positrons generated in a positron production target through a Capture Linac (CL). It raises a question of how to manage their large 6D phase space to provide bunches matched to the damping ring acceptance. This paper presents the beam dynamics studies of the FCC-ee positron linac consisting of an Adiabatic Matching Device (AMD) with theoretical field distribution combined with constant solenoidal field along  $9/10\pi$  large aperture L-band accelerating structures. AMD field drop rate, as well as the RF field phase and accelerating structure length, were varied to find features of a bunch formation. It was shown that 5D normalized beam brightness is a useful parameter to optimize the initial part of the CL. A higher beam brightness can be obtained for the higher AMD field drop rate. Two peak structure appears in the normalized brightness dependence on the RF field phase. The peaks correspond to the acceleration of the head or the tail of the initial positron longitudinal distribution. The last one provides a higher positron yield.

## INTRODUCTION

The Future electron-positron Circular Collider, FCC-ee, requires an intense positron beam [3, 4]. In all positron sources used for accelerators, positrons are produced as secondary beams from an electromagnetic shower cascade generated by high-energy electrons impinging on a target made of high-Z material, which provides relatively high conversion efficiency. The resulting final 6D normalized emittance is huge due to large transverse and longitudinal momentum spreads of positrons caused by shower processes and multiple scattering in the target. At the same time, produced positron bunches are small in transverse and longitudinal directions. Accommodation of these bunches to the acceptance of an adjacent accelerator, mandates the reduction of angular spread. A special focusing magnet, so-called matching device, must provide a strong axial (or azimuthal) magnetic field of the order of several Tesla with a peak near the target (ideally at its output surface) that drops to a constant value, typically below 0.5 T for the reduction of the transverse momentum of the particles increasing their longitudinal momentum (see [5]). Particle trajectories lengthening after the match-

ing device results in bunch size increase both transverse and longitudinal. Therefore, it is necessary to place an accelerating structure with enough large aperture just after the matching device to accommodate a maximum number of particles as well as to manipulate the longitudinal phase space to bunch them. Obtaining short bunches at the initial stage of acceleration is essential for low energy spread of the beam at the exit of the positron linac.

The aim of this work is to find features of a bunch formation in a positron CL with a layout mostly based on that described in [6]. In the simulations, the field drop rate of the matching device, as well as the RF field phase and accelerating structure length were varied. The results of the simulation are presented below.

## SIMULATION TECHNIQUE

Tracking of particles from positron generating target through positron accelerator was performed with the Astra (A Space Charge Tracking Algorithm) program package [7]. Initial positron distribution at the exit of the target was the same as that used in [6] obtained with GEANT4 [8] simulation of the interaction between the primary 6 GeV electron beam and the 17.5 mm tungsten target. The parameters of the positron beam at the target exit are listed in Table 1.

Table 1: Initial positron beam parameters

Parameter	Value	Units
Positron yield	13.6	$n_{e^+}/n_{e^-}$
Beam sizes $\sigma_x, \sigma_y$	1.3	mm
rms emission time $\sigma_t$	4.4	ps
Average kinetic energy	50.54	MeV
Energy spread	123	MeV
Transverse beam emittances	$1.9 \cdot 10^4$	$\pi \cdot \text{mm} \cdot \text{mrad}$

To study the influence of the field drop rate of the matching device on beam performance, axial on-axis magnetic field was represented in a form of superposition of the AMD field [9] and constant solenoidal field  $B_{sol}$

$$B_z(z) = \frac{B_0}{1+\alpha z} + B_{sol} \quad (1)$$

where  $z$  is an axial coordinate,  $B_0$  is a field magnitude at the front end of the AMD at  $z = 0$ ,  $\alpha$  is a tapering parameter. The study was carried out in two stages. At first,  $B_0 = 12$  T and  $B_{sol} = 0.5$  T were fixed to investigate the influence of  $\alpha$  in the range of  $10 \text{ m}^{-1}$  to  $60 \text{ m}^{-1}$  on positron beam performance.

\* Work supported by ANR (Agence Nationale de la Recherche) Grant No: ANR-21-CE31-0007 and was done under CHART Collaboration (Swiss Accelerator Research and Technology, <http://www.chart.ch>).

† mytrochenko@ijclab.in2p3.fr

There are two options to represent the accelerating structure in the Astra code. For the first (default) option traveling wave field is derived from a standing wave field map that contains an integer number of wavelengths and field of two couplers. For the  $9/10\pi$  structure that number corresponds to twenty cells so accelerating structure length can be changed with 20 cell steps. To have a less coarse step of structure length change traveling wave field of an accelerating structure with any number of cells can be represented as a superposition of field maps of its real and imaginary parts.

Two options of CL layout were considered.

- The  $9/10\pi$  structure containing 60 cells and two couplers was placed downstream of the target in such a way that distance  $d$  from the target exit face to the structure input coupler centre was 0.33 m. The influence of the field drop rate of the matching device, as well as the RF field phase on beam parameters was studied. Then, the CL with four such accelerating structures was considered.
- The  $9/10\pi$  structure of variable number of cells from 28 through 112 including the two couplers was placed downstream of the target in such a way that  $d=0.36$  m. The influence of accelerating structure length was studied.

Beam 5D normalized brightness  $B_{nrms}$  was taken as a figure of merit for the simulations because it combines three most important values for the injector part of a linac, namely: bunch phase length  $\Delta\Phi$ , bunch charge  $Q_p \cdot N_p$  and transverse emittances  $\varepsilon_{nxrms}, \varepsilon_{nyrms}$ .

$$B_{nrms} = \frac{2I}{\varepsilon_{nxrms} \varepsilon_{nyrms}}, \quad (2)$$

$$2I \propto 360^\circ \cdot Q_p \cdot f_0 \frac{N_p}{\Delta\Phi}, \quad (3)$$

where  $Q_p$  is macroparticle charge and  $N_p$  is the number of macroparticles in an output bunch.

To estimate the accepted positron yield, the longitudinal phase space of particles was cropped by longitudinal acceptance of the Dumping Ring (DR):  $\pm 3.8\%$  at 1.540 GeV in energy and 16.7 mm in longitudinal dimension. To bring the longitudinal phase space from CL exit to the energy of the DR the LiTrack [10] style formula was used:  $W_{dr} = W + (1.54 - W_0) \cos(\varphi + 2\pi(z - z_0))$ , where  $W_{dr}$  and  $W$  are particle energies at the DR level and at the CL exit respectively,  $W_0$  and  $z_0$  correspond to peaks of energy and longitudinal spreads of particles at the CL exit respectively, while  $\varphi$  is RF phase offset from the wave crest.

## RESULTS OF SIMULATION AND DISCUSSION

To show the influence of  $\alpha$  in Eq. (1) on the bunch parameters in general, the first layout was simulated with the accelerating structure phase set for maximum acceleration. The amplitude of the field was set to get maximum

energy gain of 30 MeV. The maximum field in AMD was 12.5 T. Results are shown in Fig. 1 (left). One can see that at slow field drop more positrons are collected, but the phase length of the bunch is larger because of the bunch lengthening. It should be noted that the transverse emittance is lower with greater particle loss.

To find how these values interplay at different field phases simultaneous scans on  $\alpha$  and the field phase were performed at a higher accelerating gradient (maximum energy gain was 62 MeV). The results are shown in Fig. 1 (right).

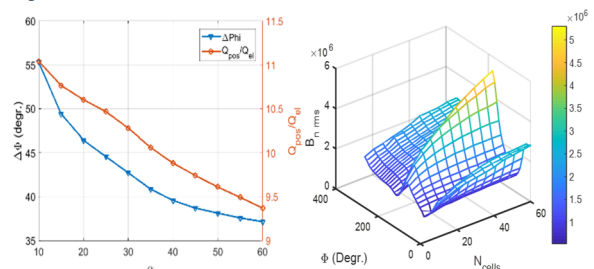


Figure 1: Total positron yield and bunch phase length vs. tapering parameter  $\alpha$  (left). Normalized brightness vs.  $\alpha$  and field phase (right).

The dependence of the brightness on the field phase has two ridges that grow with increasing  $\alpha$ . The highest peak corresponds to the acceleration of the initial bunch tail and the other one to the acceleration of the head of the bunch. Analysis of the particle dynamics showed that at the maximum brightness the first RF bucket contains 99% of the particles.

Three more accelerating structures were placed downstream of the first one with a distance between adjacent coupler centers of 0.35 m. The beam from the first structure at maximum brightness was used as input to that part of the linac but the reference particle was moved to the new bunch center. Phases of the three structures were set for maximum acceleration but with a phase offset of  $-15^\circ$  to provide some additional longitudinal compression of the bunch.

Figure 2 shows resulted longitudinal phase space cropped at the DR level. The accepted yield is  $8.0 n_{e^+}/n_{e^-}$  and the total yield is  $8.6 n_{e^+}/n_{e^-}$ . The root mean square (RMS) energy spread of accepted particles  $\Delta W/W$  is 1.1% and RMS bunch length  $\Delta Z$  is 2.8 mm.

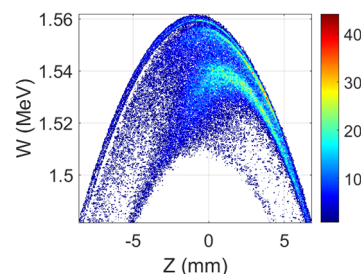


Figure 2: Longitudinal phase space at the DR level.

To show how accelerating structure length influences beam bunching, scan of the RF field phase for the structures containing different number of cells was carried out

at  $\alpha = 60 \text{ m}^{-1}$ . The result is shown in Fig. 3 (left) for the maximum acceleration gradient of 16 MeV/m. Shown dependence has a two-ridge structure. The ridges correspond to the acceleration of the head or the tail of the initial positron longitudinal distribution. The last one provides the higher positron yield for the longer structures. Although the figure does not show an optimal structure length, calculations have indicated a decrease in acceptable yield after a length of 100 cells. Figure 3 (right) shows longitudinal phase space cropped by  $\pm 3.8\%$  at 1.54 GeV. The length of the cut window is 16.7 mm in this case. The accepted yield is 8.3,  $1\sigma \Delta W/W$  is 1.03% and  $1\sigma \Delta Z = 2.48 \text{ mm}$ .

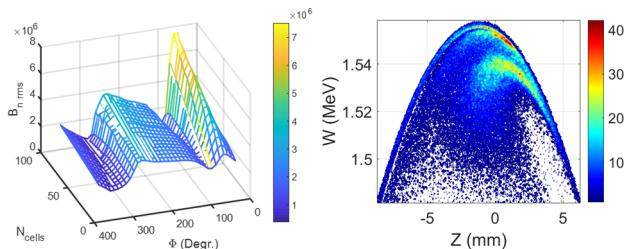


Figure 3: Normalized brightness vs the structure length and field phase (left) and longitudinal phase space at the DR level (right).

Evolution of positron longitudinal phase space along the linac with 112-cell accelerating structure is shown in Fig. 4. The actual distance between adjacent distributions is 1 m. For the convenience of presentation, the distributions artificially shifted back and placed with a period of a half of wavelength. High-energy particles at the head of the bunch are cut off on graphs. One can see that particles occupied the first RF bucket. Calculations showed that it contains at least 99% of the whole beam distribution. RF phase is set to accelerate a tail of the initial bunch, so phase space is rotating along the linac that leads to the short bunch formation. Then, RF phase must be readjusted to accelerate dense part of the bunch on a RF wave crest in the downstream linac.

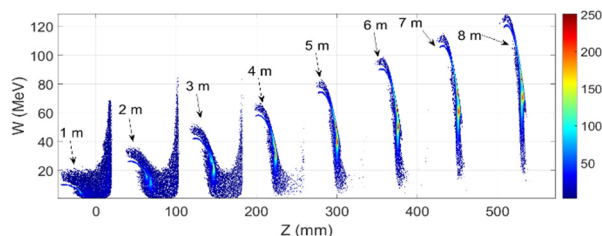


Figure 4: Longitudinal phase space along the linac. Numbers above graphs correspond to distance from the positron target in meters.

The 100-cell length accelerating structure with phase advance  $9/10\pi$  per cell is a rather long both from manufacturing and filing time point of view. Therefore, we simulate two 50-cell (3.61 m) length accelerating structures. Obtained results are almost the same as for one long structure: accepted yield is  $8.2 n_{e^+}/n_{e^-}$ ,  $1\sigma \Delta W/W$  is 1.09% and  $1\sigma \Delta Z = 2.67 \text{ mm}$ . Slight difference in beam parameters is probably due to the influence of two additional couplers in such a layout.

Table 2 summarizes the best results obtained in this study with comparison of that for the FCC-ee capture linac Version 0 numbers (see [11], Table 10). It seems that beam parameters of the FCC-ee capture linac Version 0 can be enhanced. Analysis shows the main difference between these cases is in magnetic field configuration in the region from the target-converter to the linac entrance. The magnetic field configuration should provide suitable bunch lengthening to keep particles within one RF bucket during longitudinal phase space rotation allowing short bunch formation.

Table 2: Positron beam parameters and its comparison to parameters of CL Version 0

Parameter	This study	FCC-ee V0	Units
Maximum accelerating gradient	16	20	MeV/m
Mean energy at DR entrance	1.54	1.54	GeV
$1\sigma \Delta W/W$ at DR entrance	1.0	1.6	%
$1\sigma \Delta Z$ at DR entrance	2.5(6.0)	3.0(7.2)	mm ( $^\circ$ )
Accepted positron yield	8.3	6.6	$n_{e^+}/n_{e^-}$
$\epsilon_{n \text{ rms } x,y}$	13	13	mm-rad

## CONCLUSION

The beam dynamics of the FCC-ee positron capture linac consisting of the AMD with theoretical field distribution combined with constant solenoidal field along  $9/10\pi$  large aperture L-band accelerating structures have been studied. AMD field drop rate, as well as the RF field phase and accelerating structure length can be optimized to provide short bunch formation within one RF bucket with the accepted positron yield of  $8.3 n_{e^+}/n_{e^-}$ . It is necessary to study the feasibility of the magnetic field profile obtained in current studies.

## ACKNOWLEDGEMENTS

The authors would like to thank Yongke Zhao from CERN and Mattia Schaer from PSI for provided data and useful discussions. The first author would like to thank PAUSE-ANR Ukraine Program for financial support.

## REFERENCES

- [1] N. Vallis, B. Auchmann, P. Craievich, *et al.* “The PSI positron production project”. in *Proc. 31th Linear Accelerator Conf. (LINAC’22)*, Liverpool, UK, Aug. – Sep. 2022, pp. 577 – 580. doi:10.18429/JACoW-LINAC2022-TUPORI16
- [2] H. W. Pommerenke *et al.*, “RF design of traveling-wave accelerating structures for the FCCee injector complex”. in *Proc. 31th Linear Accelerator Conf. (LINAC’22)*, Liverpool, UK, Aug. – Sep. 2022, pp. 707 – 710. doi:10.18429/JACoW-LINAC2022-THPOJ008

- [3] A. Abada *et al.*, The European Physical Journal Special Topics 228, 261 (2019).
- [4] I. Chaikovska *et al.*, “Positron Source for FCC-ee”, in *Proc. IPAC'19*, Melbourne, Australia, May 2019, pp. 424-427. doi:10.18429/JACoW-IPAC2019-MOPMP003
- [5] I. Chaikovska *et al.*, “Positron sources: from conventional to advanced accelerator concepts-based colliders”, *J. Instrum.* vol. 17, no. 5, pp. P05015, 2022. doi:10.1088/1748-0221/17/05/p05015
- [6] Y. Zhao, S. Doebert, A. Latina, *et al.* “Optimization of the FCC-ee positron source using a HTS solenoid matching device”. In *Proc of 13th Int. Particle Acc. Conf. (IPAC'22)*, Bangkok, Thailand, June 2022, pp. 2003 – 2006. doi:10.18429/JACoW-IPAC2022-WEPOPT062
- [7] K. Flottmann, S. M. Lidia, P. Piot, “Recent improvements to the Astra particle tracking code”. In *Proc. of the 2003 Particle Acc. Conf. (PAC2003)*, May 2003, Portland, Oregon, pp. 3500 – 3502.
- [8] S. Agostinelli *et al.*, “GEANT4: A Simulation toolkit”, *Nucl. Instrum. Meth.*, Vol. A506, pp. 250–303, 2003. doi:10.1016/S0168-9002(03)01368-8
- [9] R. Chehab, “Positron sources”, LAL/RT 92-17 (1992).
- [10] K.L.F. Bane, P. Emma, “LiTrack: a fast longitudinal phase space tracking code with graphical user interface”. In *Proc. of the 2005 Particle Acc. Conf. (PAC2005)*, May 2005, Knoxville, Tennessee, pp. 4266 – 4268.
- [11] S. Bettoni, P. Craievich, J.-Y. Raguin, *et al.* “FCC-ee Injector Study and the P3 Project at PSI”. CHART Scientific Report 2022, URL: <https://chart.ch/wp-content/uploads/2023/02/FCce-Injector-2022.pdf>